http://dx.doi.org/10.5012/bkcs.2012.33.11.3772

Virtual Screening and Biochemical Evaluation of Mitogen-activated Protein Kinase Phosphatase 4 Inhibitors

Hwangseo Park,[*] Jeong-Yi Jeon,[†] and Seong Eon Ryu[†,*]

Department of Bioscience and Biotechnology, Sejong University, Seoul 143-747, Korea. [*]E-mail: hspark@sejong.ac.kr
[†]Department of Bioengineering, Hanyang University, Seoul 133-791, Korea. [*]E-mail: ryuse@hanyang.ac.kr
Received August 2, 2012, Accepted August 27, 2012

Mitogen-activated protein kinase phosphatase 4 (MKP4) has proved to be a promising target for the development of therapeutics for the treatment of diabetes and the other metabolic diseases. Here, we report an example for a successful application of the structure-based virtual screening to identify three novel inhibitors of MKP4. These inhibitors have desirable physicochemical properties as a drug candidate and reveal a moderate potency with IC_{50} values ranging from 4.9 to 32.3 μM. Therefore, they deserve consideration for further development by structure-activity relationship studies to optimize the inhibitory and antidiabetic activities. Structural features relevant to the stabilization of the newly identified inhibitors in the active site of MKP4 are discussed in detail.

Key Words : Virtual screening, Docking, MKP4, Inhibitor, Antidiabetic agents

Introduction

The respective roles of phosphorylation and dephosphorylation played by protein tyrosine kinases and protein tyrosine phosphatases (PTPs) are the hallmarks of cellular signal transduction.[1] Among the 107 members of PTP superfamily identified in the human genome, 61 belong to dual-specificity phosphatase (DUSP)[2] that has a characteristic structure of the catalytic domain. Some DUSPs exhibit a dual dephosphorylation activity with respect to mitogen-activated protein kinases (MAPKs) and thereby regulate the cellular signal transduction pathways associated with growth, differentiation, motility, metabolism, apoptosis, and immune responses. This mitogen-activated protein kinase phosphatase (MKP) subset of DUSP has 11 members, all of which contain not only a catalytic domain but also a MAPK-binding domain in the N-terminal region.[3]

The MKP subset includes MKP4 that has a broad specificity toward three MAPK substrates: extracellular signal-regulated kinase (ERK), c-Jun N-terminal kinase (JNK), and p38.[4] Although MKP4 is expressed in insulin-sensitive tissues, it was also shown to be overexpressed in obese insulin-resistant rodent models.[5] This indicates that MKP4 should be a promising therapeutic target for the treatment of diabetes and obesity. Three dimensional (3D) structures of MKP4 were also reported both in the resting form and in complex with a substrate analogue.[6,7] The presence of structural information about the nature of the active site and the interactions with a small-molecule ligand can make it a plausible task to design the potent inhibitors that may develop into a drug candidate. Indeed, the usefulness of such structural information has been well appreciated in designing the potent and selective small-molecule inhibitors of various phosphatases.[8] Nonetheless, the discovery of MKP4 inhibitors has lagged behind the biochemical and structural studies. Only a few classes of MKP4 inhibitors has been reported so far, which were shown to bind at an allosteric site instead of the active site.[7]

In the present study, we identify the novel classes of MKP4 inhibitors by means of a structure-based drug design protocol involving the virtual screening with docking simulations and *in vitro* enzyme assay. The characteristic feature that disciriminates our virtual screening approach from the others lies in the implementation of an accurate solvation model in calculating the binding free energy between MKP4 and the putative ligands, which would have an effect of increasing the hit rate in enzyme assay.[9] We find in this study that the docking simulations with the improved binding free energy function can be a useful computational tool for elucidating the activities of the identified inhibitors, as well as for enriching the chemical library with molecules that are likely to have desired biological activities.

Methods

X-ray crystal structure of MKP4 reported by Almo *et al.* (PDB entry: 2HXP)[7] was used as the receptor model in the virtual screening with docking simulations. A special attention was paid to assign the protonation states of the ionizable Asp, Glu, His, and Lys residues in the X-ray structure of MKP4. The side chains of Asp and Glu residues were assumed to be neutral if one of their carboxylate oxygens pointed toward a hydrogen-bond accepting group including the backbone aminocarbonyl oxygen at a distance within 3.5 Å, a generally accepted distance limit for a hydrogen bond of moderate strength.[10] Similarly, the lysine side chains were assumed to be protonated unless the NZ atom was in proximity of a hydrogen-bond donating group. The same procedure was also applied to determine the protonation states of ND and NE atoms in His residues.

The docking library for MKP4 comprising about 240,000 compounds was constructed from the latest version of the chemical database distributed by Interbioscreen (http://www.ibscreen.com) containing approximately 477,000 synthetic and natural compounds. Prior to the virtual screening with docking simulations, they were filtrated on the basis of Lipinski's "Rule of Five" to adopt only the compounds with the physicochemical properties of potential drug candidates[11] and without reactive functional group(s). All of the compounds included in the docking library were then processed with the CORINA program to generate their 3D atomic coordinates, followed by the assignment of Gasteiger-Marsilli atomic charges.[12] We used the AutoDock program[13] in the virtual screening of MKP4 inhibitors because the outperformance of its scoring function over those of the others had been shown in several target proteins.[14] Docking simulations with AutoDock were then carried out in the active site of MKP4 to score and rank the compounds in the docking library according to their calculated binding affinities.

In the actual docking simulation of the compounds in the docking library, we used the empirical AutoDock scoring function improved by the implementation of a new solvation model for a compound. The modified scoring function has the following form:

$$\Delta G_{bind}^{aq} = W_{vdW}\sum_{i=1}\sum_{j=1}\left(\frac{A_{ij}}{r_{ij}^{12}}-\frac{B_{ij}}{r_{ij}^{6}}\right) + W_{hbond}\sum_{i=1}\sum_{j=1}E(t)\left(\frac{C_{ij}}{r_{ij}^{12}}-\frac{D_{ij}}{r_{ij}^{10}}\right) + W_{elec}\sum_{i=1}\sum_{j=1}\frac{q_i q_j}{\varepsilon(r_{ij})r_{ij}} + W_{tor}N_{tor} + W_{sol}\sum_{i=1}S_i\left(O_i^{\max}-\sum_{j\neq i}V_j e^{-\frac{r_{ij}^2}{2\sigma^2}}\right), \quad (1)$$

where W_{vdW}, W_{hbond}, W_{elec}, W_{tor}, and W_{sol} are the weighting factors of van der Waals, hydrogen bond, electrostatic interactions, torsional term, and desolvation energy of inhibitors, respectively. r_{ij} represents the interatomic distance, and A_{ij}, B_{ij}, C_{ij}, and D_{ij} are related to the depths of the potential energy well and the equilibrium separations between the two atoms. The hydrogen bond term has an additional weighting factor, $E(t)$, representing the angle-dependent directionality. Cubic equation approach was applied to obtain the dielectric constant required in computing the interatomic electrostatic interactions between MKP4 and a ligand molecule.[15] In the entropic term, N_{tor} is the number of rotatable bonds in the ligand. In the desolvation term, S_i and V_i are the solvation parameter and the fragmental volume of atom i,[16] respectively, while $O_i^{\max}$ stands for the maximum atomic occupancy. In the calculation of molecular solvation free energy term in Eq. (1), we used the atomic parameters developed by Kang *et al.*[17] This modification of the solvation free energy term is expected to increase the accuracy in virtual screening because the underestimation of ligand solvation often leads to the overestimation of the binding affinity of a ligand with many polar atoms.[9] Indeed, the superiority of this modified scoring function to the previous one was well-appreciated in recent studies for virtual screening of kinase and phosphatase inhibitors.[18,19]

The catalytic domain of human MKP4 (MKP4C, residues 201-351) was subcloned into pET28a and overexpressed using *Escherichia coli* BL21 (DE3) strain. Cells were grown at 18 °C after induction with 0.1 mM IPTG for 16 h. His-tagged MKP4C was purified by nickel-affinity chromatography and dialyzed against the buffer containing 20 mM Tris-HCl (pH 8.0), 0.2 M NaCl, and 5 mM DTT. 92 compounds selected from the precedent virtual screening were evaluated for their *in vitro* inhibitory activity against the recombinant MKP4C. Assays were performed by monitoring the extent of hydrolysis of 6,8-difluoro-4-methyl-umbelliferyl phosphate (DiFMUP) with a spectrofluorometric assay. The purified MKP4C (5 nM), DiFMUP (10 μM) and a candidate inhibitor were incubated in the reaction mixture containing 20 mM Tris-HCl (pH 8.0), 0.01% Trition X-100, and 5 mM DTT for 20 minutes. This enzymatic reaction was stopped with the addition of sodium orthovanadate (1 mM). The phosphatase activities were then checked by the absorbance changes due to the hydrolysis of the substrate at 460 nm. To determine the IC_{50} values of the inhibitors, their inhibitory activities were measured in duplicate at the concentrations of 0.0, 1.0, 2.0, 5.0, 10, 20, and 50 μM to obtain the dose-response curve fits. IC_{50} values of the inhibitors were then determined from direct regression analysis using the four-parameter sigmoidal curve as implemented in the SigmaPlot program.

Results and Discussion

Of the 240,000 compounds screened with docking simulations in the active site of MKP4, 100 top-scored compounds were selected as virtual hits. 92 of them were available from the compound supplier and were tested for inhibitory activity against MKP4 by *in vitro* enzyme assay. As a result, we identified three compounds that inhibited the catalytic activity of MKP4 by more than 50% at the concentration of 50 μM, which were selected to determine the IC_{50} values. We note that the hit rate of virtual screening is as low as 3%. This is actually not surprising because the design of new DSP phosphatase inhibitors has been very difficult due to the flat and shallow active site that prevents the inhibitors from being fully accommodated.[20] The chemical structures and the inhibitory activities of the newly identified inhibitors are shown in Figure 1 and Table 1, respectively. It is a common feature in the molecular structures of three identified

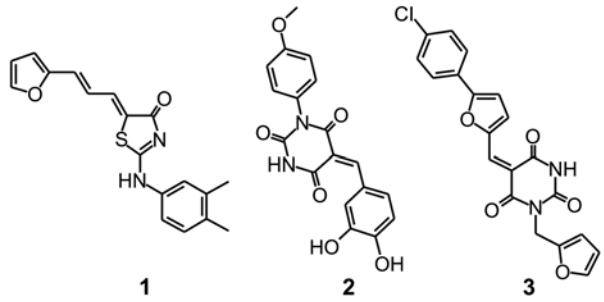

Figure 1. Chemical structures of the newly identified MKP4 inhibitors.

Table 1. IC_{50} values (in μM) of **1-3** against MKP4, MKP1, MKP7, and MKP-X

Compounds	MKP4	MKP1	MKP7	MKP-X
1	4.9	> 100	> 100	> 100
2	25.9	> 100	> 100	> 100
3	32.3	> 100	32.6	> 100

inhibitors that a heterocycle group involving the carbonyl moiety flanks the terminal aromatic rings. To the best of our knowledge, none of these compounds have been reported as MKP inhibitors so far, and no additional biological activity was found at least in the two most public chemical databases, ChEMBL and PubChem. As can be seen in Table 1, the three inhibitors reveal a moderate potency against MKP4 with the associated IC_{50} values of ranging from 4.9 to 32.3 μM. Because the inhibitors cannot be fully accommodated in the active site, **1-3** are likely to be capable of establishing strong multiple hydrogen bonds with the active-site resides of MKP4. Because these inhibitors were also screened for having desirable physicochemical properties as a drug candidate, they deserve consideration for further development by structure-activity relationship (SAR) studies to optimize the inhibitory activity.

Because the selectivity has been one of the most important issues in the development of phosphatase inhibitors, we also determined the inhibitory activities of **1-3** for some other MKPs including MKP1, MKP7, and MKP-X. As can be seen in Table 1, all three MKP4 inhibitors reveal lower potencies for the three other MKPs than for MKP4 although **3** appears to be almost equipotent for MKP7. In particular, **1** and **2** are found to be almost inactive against the three other MKPs. Thus, the inhibitors **1-3** seem to bind in the active site of MKP4 in a stronger fashion than in those of the other structurally similar MKPs. These selectivities of the identified inhibitors also indicate that they would impair the enzymatic activity of MKP4 through the non-bond interactions in the active site instead of making a covalent bond with the side-chain thiolate ion of the catalytic cysteine residue contained in most of MKPs in common.

In order to get structural insight into the inhibitory mechanisms of the identified MKP4 inhibitors, we investigated their binding modes in the active in a comparative fashion. Figure 2 shows the lowest-energy conformations of **1-3** in active site gorge of MKP4 calculated with the modified AutoDock program. The results of these docking simulations are self-consistent in the sense that the functional groups of similar chemical character are placed in similar ways with comparable interactions with the protein groups. As revealed by the superposition of their docked structures, for example, the functional groups that serve as a surrogate for the substrate phosphotyrosine group (furan and benzene-1,2-diol moieties) are directed to the catalytic cystein residue (Cys290) while the hydrophobic groups point toward the WPD loop above the active site. These common features in the calculated binding modes indicate that an effective MKP4 inhibitor should include a surrogate for the substrate phosphotyrosine

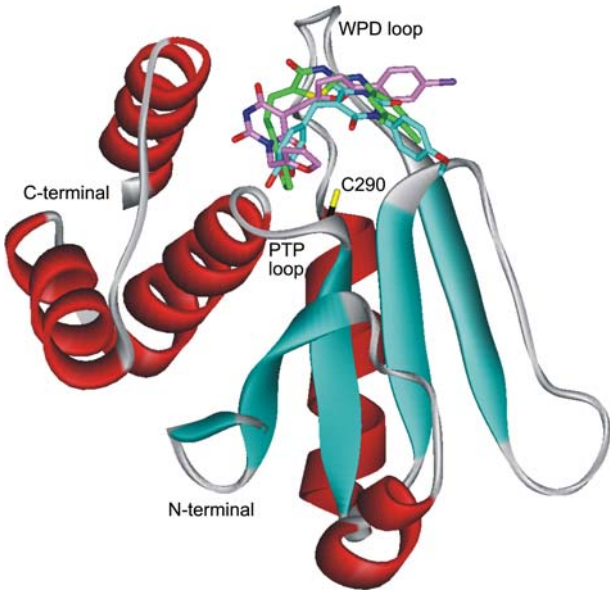

Figure 2. Comparative view of the binding modes **1-3** in the active site of MKP4. Carbon atoms of **1**, **2**, and **3** are indicated in green, cyan, and pink, respectively. The positions of PTP loop, WPD loop, and the catalytic residue Cys290 are also indicated.

group and simultaneously the hydrophobic groups for binding to the WPD loop. In order to examine the possibility of the allosteric inhibition of MKP4 by the identified inhibitors, docking simulations were carried out with the grid maps for the receptor model so as to include the entire part of its catalytic domain. However, the binding configuration in which an inhibitor resides outside the active site was not observed for any of the new inhibitors. These results support the possibility that **1-3** would impair the catalytic activity of MKP4 through the specific binding in the active site.

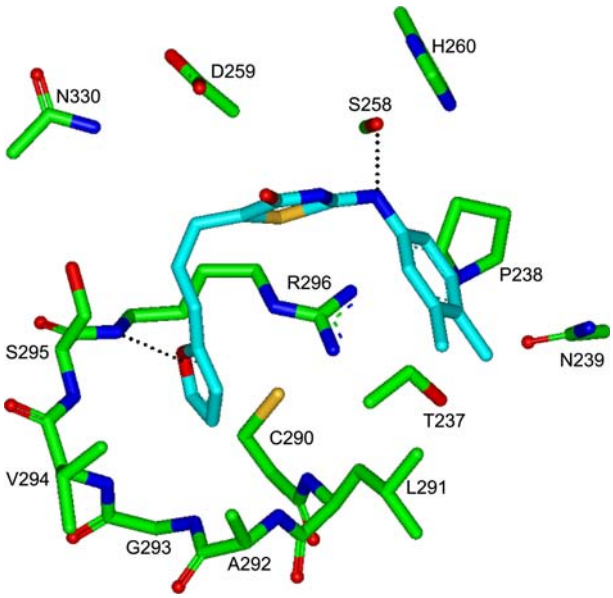

Figure 3. Calculated binding mode of **1** in the active site of MKP4. Carbon atoms of the protein and the ligand are indicated in green and cyan, respectively. Each dotted line indicates a hydrogen bond.

The calculated binding mode of **1** in the active site of MKP4 is shown in Figure 3. It is noted that the oxygen atom on the furan ring of the inhibitor receives a hydrogen bond from the backbone amidic group of Arg296. A similar hydrogen bond was also observed in the X-ray crystal structure of MKP4 in complex with a substrate analogue of the phosphate ion.[7] Apparently, this hydrogen bond should serve as an anchor for positioning the inhibitor at the active site. It is also noteworthy that the furan ring of the inhibitor resides in the vicinity of the side-chain thiolate ion of Cys290 with the associated interatomic distances of 3-5 Å. These distances are very similar to that between the phosphorous atom of the substrate analogue and the side chain of Cys290 of MKP4 (3.41 Å) in the X-ray crystal structure.[7] Judging from the proximity to Cys290 and the formation of a hydrogen bond in the active site, the furan ring seems to be an effective surrogate for the substrate phosphate group. A stable hydrogen bond is also established between the -NH- group of the inhibitor and the side-chain hydroxy group of Ser258, which should also be a significant binding force to stabilize the MKP4-**1** complex. The inhibitor **1** can be further stabilized in the active site by the hydrophobic interactions of its nonpolor groups with the side chains of Pro238, His260, Leu291, Ala292, and Val294. Thus, the overall structural features derived from docking simulations indicate that the micromolar inhibitory activity of **1** stems from the multiple hydrogen bonds and hydrophobic interactions established simultaneously in the active site. **1** is expected to serve as a good inhibitor scaffold from which much more potent inhibitors can be derivatized because of its low molecular weight of ~324.

Figure 4 shows the lowest-energy binding mode of **2** in the active site of MKP4. The binding mode of **2** is similar to that of **1** in that the roles of hydrogen bond donor with respect to the benzene-1,2-diol moiety are played by the backbone amide groups of Arg296 and Val294 that reside at the bottom of the active site. One of the aminocarbonyl oxygens in the pyrimidine-2,4,6-trione group of **2** forms an additional hydrogen bond with the backbone amidic nitrogen of Ser258, which should also play a significant role in stabilizing the inhibitor in the active site. Hydrophobic interactions in the MKP4-**2** complex are established also in a similar fashion to that in the MKP4-**1** complex: its two phenyl rings form the van der Waals contacts with the side chains of Pro238, Leu240, His260, Leu291, Ala292, and Val294. It is worth noting that the number of hydrogen bonds increases from two in the MKP4-**1** to three in the MKP4-**2** complex, which would have an effect of enhancing the inhibitory activity. On the other hand, the solvation free energy of **2** is found to be lower than that of **1** by 3.6 kcal/mol due to the presence of more polar groups in the former than in the latter. The gain of one additional hydrogen bond seems to be insufficient to compensate for the increase in desolvation cost for the enzyme-inhibitor complexation, which can be invoked to explain the lower inhibitory activity **2** than **1**. This indicates that in order to enhance the potency of an inhibitor with a structural change, the resulting increase in the strength of enzyme-inhibitor interaction should be sufficient to surmount the increased stabilization in solution.

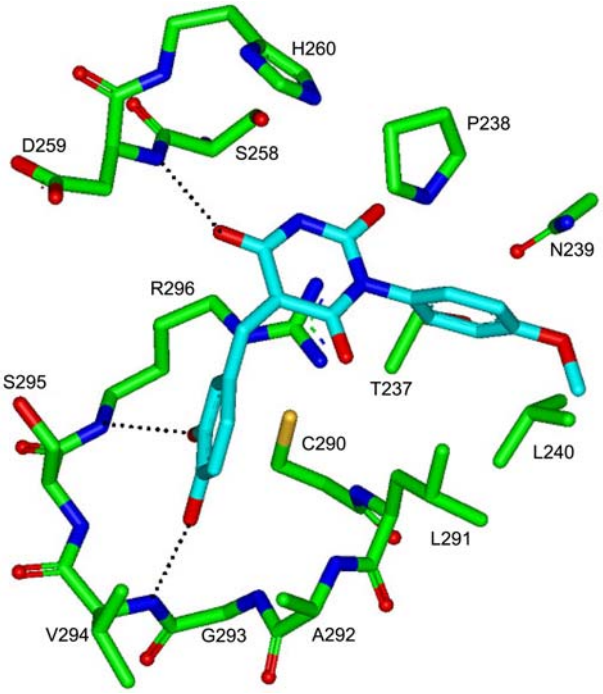

Figure 4. Calculated binding mode of **2** in the active site of MKP4. Carbon atoms of the protein and the ligand are indicated in green and cyan, respectively. Each dotted line indicates a hydrogen bond.

Conclusions

In summary, we have identified three novel inhibitors of MKP4 by applying a computer-aided drug design protocol involving the structure-based virtual screening with docking simulations under consideration of the effects of ligand solvation in the scoring function. These inhibitors have desirable physicochemical properties as a drug candidate and reveal a moderate potency with the associated IC_{50} values ranging from 4.9 to 32.3 μM. Therefore, each of the newly discovered inhibitors deserves consideration for further development by SAR studies to optimize the inhibitory and antidiabetic activities. Detailed binding mode analyses with docking simulations show that the inhibitors can be stabilized in active site by the simultaneous establishment of multiple hydrogen bonds and van der Waals contacts.

Acknowledgments. This work was supported by Basic Science Research Program through the National Research Foundation of Korea (NRF) funded by the Ministry of Education, Science and Technology (2011-0022858), and a Hanyang University internal grant.

References

1. Tonks, N. K. *Nature Rev. Mol. Cell Biol.* **2006**, *7*, 833.
2. Alonso, A.; Sasin, J.; Bottini, N.; Friedberg, I.; Friedberg, I.;

Osterman, A.; Godzik, A.; Hunter, T.; Dixon, J.; Mustelin, T. *Cell* **2004**, *117*, 699.
3. Farooq, A.; Zhou, M. M. *Cell Signal.* **2004**, *16*, 767.
4. Muda, M.; Boschert, U.; Smith, A.; Antonsson, B.; Gillieron, C.; Chabert, C.; Camps, M.; Martinou, I.; Ashworth, A.; Arkinstall, S. *J. Biol. Chem.* **1997**, *272*, 5141.
5. Xu, H.; Dembski, M.; Yang, Q.; Moriarty, A.; Tayber, O.; Chen, H.; Kapeller, R.; Tartaglia, L. A. *J. Biol. Chem.* **2003**, *278*, 30187.
6. Jeong, D. G.; Yoon, T. S.; Jung, S.-K.; Park, B. C.; Park, H.; Ryu, S. E.; Kim, S. J. *Acta Cryst.* **2011**, *D67*, 25.
7. Almo, S. C.; Bonanno, J. B.; Sauder, J. M.; Emtage, S.; Dilorenzo, T. P.; Malashkevich, V.; Wasserman, S. R.; Swaminathan, S.; Eswaramoorthy, S.; Agarwal, R.; Kumaran, D.; Madegowda, M.; Ragumani, S.; Patskovsky, Y.; Alvarado, J.; Ramagopal, U. A.; Faber-Barata, J.; Chance, M. R.; Sali, A.; Fiser, A.; Zhang, Z. Y.; Lawrence, D. S.; Burley, S. K. *J. Struct. Funct. Genomics* **2007**, *8*, 121.
8. Hayashi, R.; Tanoue, K.; Durell, S. R.; Chatterjee, D. K.; Jenkins, L. M.; Appella, D. H.; Appella, E. *Biochemistry* **2011**, *50*, 4537.
9. Shoichet, B. K.; Leach, A. R.; Kuntz, I. D. *Proteins* **1999**, *34*, 4.
10. Jeffrey, G. A. *An Introduction to Hydrogen Bonding*; Oxford University Press: Oxford, 1997.
11. Lipinski, C. A.; Lombardo, F.; Dominy, B. W.; Feeney, P. J. *Adv. Drug Delivery Rev.* **1997**, *23*, 3.
12. Gasteiger, J.; Marsili, M. *Tetrahedron.* **1980**, *36*, 3219.
13. Morris, G. M.; Goodsell, D. S.; Halliday, R. S.; Huey, R.; Hart, W. E.; Belew, R. K.; Olson, A. J. *J. Comput. Chem.* **1998**, *19*, 1639.
14. Park, H.; Lee, J.; Lee, S. *Proteins* **2006**, *65*, 549.
15. Park, H.; Jeon, J. H. *Phys. Rev. E* **2007**, *75*, 021916.
16. Stouten, P. F. W.; Frömmel, C.; Nakamura, H.; Sander, C. *Mol. Simul.* **1993**, *10*, 97.
17. Kang, H.; Choi, H.; Park, H. *J. Chem. Inf. Model* **2007**, *47*, 509.
18. Park, H.; Jeon, J. Y.; Kim, S. Y.; Jeong, D. G.; Ryu, S. E. *J. Comput. Aided Mol. Des.* **2011**, *25*, 469.
19. Park, H.; Chi, O.; Kim, J.; Hong, S. *J. Chem. Inf. Model* **2011**, *51*, 2986.
20. Zhang, M.; Cho, E. J.; Burstein, G.; Siegel, D.; Zhang, Y. *ACS Chem. Biol.* **2011**, *6*, 511.